

# Electrically Tunable Magnetism in Magnetic Topological Insulators

Jing Wang, Biao Lian, and Shou-Cheng Zhang

*Department of Physics, McCullough Building, Stanford University, Stanford, California 94305-4045, USA*

(Dated: December 7, 2024)

The external controllability of the magnetic properties in topological insulators would be important both for fundamental and practical interests. Here we predict the electric-field control of ferromagnetism in a thin film of insulating magnetic topological insulators. The decrease of band inversion by the application of electric fields results in a reduction of magnetic susceptibility, and hence in the modification of magnetism. Remarkably, the electric field could even induce the magnetic quantum phase transition from ferromagnetism to paramagnetism. We further propose a topological transistor device in which the dissipationless charge transport of chiral edge states is controlled by an electric field. In particular, the field-controlled ferromagnetism in magnetic topological insulator can be used for voltage based writing of magnetic random access memories in magnetic tunnel junctions. The simultaneous electrical control of magnetic order and chiral edge transport in such devices may lead to electronic and spintronic applications for topological insulators.

PACS numbers: 73.40.-c 73.20.-r 75.70.-i 75.50.Pp

*Introduction* The recent theoretical prediction and experimental realization of the quantum anomalous Hall (QAH) effect have attracted intense interest in condensed matter physics [1–15]. The QAH insulator is a new state of quantum matter which has a topologically nontrivial electronic structure characterized by a bulk energy gap but gapless chiral edge states, leading to the quantized Hall effect without an external magnetic field [16]. The edge channels of the QAH insulator conduct without dissipation, and thus has promising potential in the applications of low-power-consumption electronic devices. In a QAH insulator, theoretically proposed for magnetic topological insulators (TIs) [3–7], the strong spin-orbit coupling and ferromagnetic (FM) ordering combine to give rise to an insulating state with a topologically nontrivial phase characterized by a finite Chern number [17]. The QAH effect has been experimentally observed in thin films of Cr-doped (Bi,Sb)<sub>2</sub>Te<sub>3</sub> magnetic TIs [12–14], where robust bulk FM is spontaneously developed in this system even in the insulating regime.

The ability to external control the magnetic properties of TIs [18–20] could be important both for fundamental and technological interest, particularly in view of recent developments in magnetoelectrics and spintronics [21, 22]. In dilute FM semiconductors, the FM is mediated by itinerant charge carriers [23] and the magnetic ordering can be tuned by controlling the carrier density through an electric field [24]. But the electrical manipulation of magnetism in *insulating* magnetic TIs has proved elusive. Recently, it has been shown that the magnetic ordering in TIs is related to the band topology [25], where the inverted band structure contributes a sizable Van Vleck magnetic susceptibility [7]. Here we propose the electric-field control of FM in a thin film of insulating magnetic TI, with an dual insulating-gate structure. The band inversion is weakened by applying an electric field, leading to a reduction of the magnetic susceptibility, which is directly related to the magnetism. Remark-

ably, the electric field could even induce a quantum phase transition from the FM phase to the paramagnetic (PM) phase. The thin film magnetic TI with strong FM exhibits the QAH effect with chiral edge states. Based on this property, we further propose a topological transistor device in which the dissipationless charge transport of topological edge states is controlled by an electric field. Such a device may lead to electronic and spintronic applications for TIs.

*Model* We begin with introducing the topological properties of a generic two-dimensional (2D) thin film of magnetic TI. For concreteness, we study the magnetically doped (Bi,Sb)<sub>2</sub>Te<sub>3</sub> family materials, where the Dirac cone of the surface states (SSs) is observed to be located in the bulk band gap. With the bulk states gapped, only the Dirac-type SSs are relevant for low energy physics in this system [7, 26]. The 2D effective Hamiltonian is

$$\begin{aligned} \mathcal{H}_0(\vec{k}) = & \epsilon(\vec{k}) + v_F k_y \sigma_1 \otimes \tau_3 - v_F k_x \sigma_2 \otimes \tau_3 \\ & + m(\vec{k}) 1 \otimes \tau_1 + V 1 \otimes \tau_3, \end{aligned} \quad (1)$$

with the basis of  $|u \uparrow\rangle$ ,  $|u \downarrow\rangle$ ,  $|l \uparrow\rangle$  and  $|l \downarrow\rangle$ , where  $u$ ,  $l$  denote the upper and lower SSs and  $\uparrow$ ,  $\downarrow$  represent the spin up and down states, respectively. For simplicity, here we ignore the particle-hole asymmetry term  $\epsilon(\vec{k})$ .  $\vec{k} = (k_x, k_y)$ .  $\sigma_i$  and  $\tau_i$  ( $i = 1, 2, 3$ ) are Pauli matrices acting on spin and layer, respectively.  $v_F$  is the Fermi velocity.  $V$  denotes the structure inversion asymmetry between the two surfaces, which may come from band-bending induced by the substrate [27], and can be tuned by applying an electric field along  $z$  direction [Fig. 4(a)].  $m(\vec{k})$  describes the tunneling effect between the upper and lower SSs. To the lowest order in  $k$ ,  $m(\vec{k}) = m_0 + m_1(k_x^2 + k_y^2)$ . For thick enough films  $m_0 = 0$ , the upper and lower SSs form gapless Dirac cones. In this case, it is suggested that these gapless Dirac SSs would mediate exchange coupling between magnetic moments

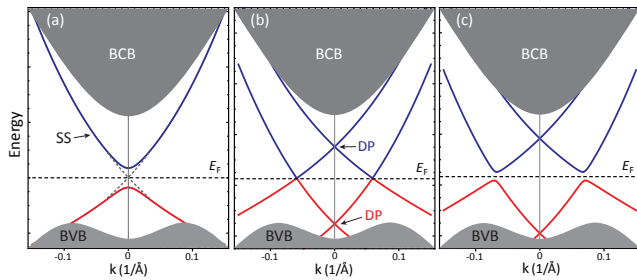


FIG. 1. (color online). Evolution of surface band structure upon increasing the structure inversion asymmetry  $V$  in thin films of a TI. The dashed line indicates the Fermi level  $E_F$ . BCB, bulk conduction band; BVB, bulk valence band; SS, surface state; DP, Dirac point. (a)  $V = 0$ , upper and lower SSs are degenerate with a hybridization gap opened at Dirac point. (b)  $V = V_c$ , upper and lower SSs move up and down in energy, respectively, and touch at a finite momentum  $k_c = V_c/v_F$ . (c)  $V > V_c$ , a band gap is reopened at  $k_c$ .

through Ruderman-Kittel-Kasuya-Yoshida (RKKY) interaction [23, 24], leading to FM in magnetic TIs [28]. For thin films  $m_0 \neq 0$ , and the coupling between these two SSs induces a hybridization gap as shown in Fig. 1(a). When the Fermi level is in the hybridized gap, the itinerant carrier mediated RKKY interaction is absent, and the Van Vleck mechanism instead takes over.

We consider in this Letter the  $m_0 \neq 0$  case, where the band topology significantly affects the magnetism of the system [25] through the Van Vleck mechanism. In terms of the new basis  $|+\uparrow\rangle$ ,  $|-\downarrow\rangle$ ,  $|+\downarrow\rangle$ ,  $|-\uparrow\rangle$  with  $|\pm\uparrow\rangle = (|u\uparrow\rangle \pm |l\uparrow\rangle)/\sqrt{2}$  and  $|\pm\downarrow\rangle = (|u\downarrow\rangle \pm |l\downarrow\rangle)/\sqrt{2}$ , the effective model becomes

$$\tilde{\mathcal{H}}_0(k_x, k_y) = \begin{pmatrix} \tilde{\mathcal{H}}_+(k) & V\sigma_1 \\ V\sigma_1 & \tilde{\mathcal{H}}_-(k) \end{pmatrix}. \quad (2)$$

Here,  $\tilde{\mathcal{H}}_{\pm}(k) = v_F(k_y\sigma_1 \mp k_x\sigma_2) + m(k)\sigma_3$ . If  $V = 0$ , this model is similar to the Bernevig-Hughes-Zhang model for HgTe quantum wells [29]. When  $m_0m_1 > 0$ , the system is a normal insulator (NI) with  $Z_2$  index  $\nu = 0$ . When  $m_0m_1 < 0$ , the system is a quantum spin Hall (QSH) insulator with  $\nu = 1$ . If  $V \neq 0$ , such inversion symmetry breaking term may induce the topological phase transition from QSH to NI [30]. The phase boundary can be determined by examining the bulk gap closing. The energy spectrum is  $E_0(k) = \pm\sqrt{(v_Fk \mp V)^2 + m^2(k)}$ , and the critical point is determined by  $m(k) = 0$  and  $v_Fk = V$  which leads to critical  $V_c = v_F\sqrt{-m_0/m_1}$ . The evolution of the band structure upon increasing the structure inversion asymmetry  $V$  is shown in Fig. 1. For  $V < V_c$ , the system is adiabatically connected to the QSH state with a full gap and  $\nu = 1$ . For  $V = V_c$ , the system is semi-metallic with gap closing at finite momentum  $k_c = V_c/v_F$ . For  $V > V_c$ , a band gap is reopened at  $k_c$  and the system is a NI.

The above discussion based on the effective model gives us a clear physical picture of the topological phase transition driven by structure inversion asymmetry. To confirm the validity of the picture and estimate the magnitude of  $V$ , we calculate the band structure of thin film  $(\text{Bi}_{0.1}\text{Sb}_{0.9})_2\text{Te}_3$  in an external electric field along  $z$  direction. We consider the three-dimensional (3D) bulk Hamiltonian  $\mathcal{H}_{3D}$  [31] in a thin film configuration with thickness  $d$ , where the effect of an external electric field is modelled by adding  $V_E(z) = \mathcal{E}z/d$ . The confinement of thin films of 3D TIs in the  $z$  direction quantizes the momentum on this axis and leads to 2D subbands. We solve the eigen equation  $[\mathcal{H}_{3D} + V_E(z)]\psi_{n\vec{k}}(z) = E_{n\vec{k}}\psi_{n\vec{k}}(z)$  with open boundary condition  $\psi_{n\vec{k}}(0) = \psi_{n\vec{k}}(d) = 0$ , where  $n$  is the subband index. By projecting the bulk model onto the lowest four subbands, the parameters in Eq. (1) for different quintuple layers (QLs) can be obtained, as shown in Table I. Each QL is about 1 nm thick. The calculated band gap for different QLs are shown in Fig. 2(a) and 2(c). Good agreement between the numerical calculation and analytic model is found, which confirms the validity of the effective model in Eq. (1). The discrepancy between them at large  $V$  suggests low energy physics is no longer dominated by Dirac-type SSs only when structure inversion asymmetry is comparable to the splitting of subbands. The energy of bulk subbands shifts little at moderate  $V$ . As is seen in Table I

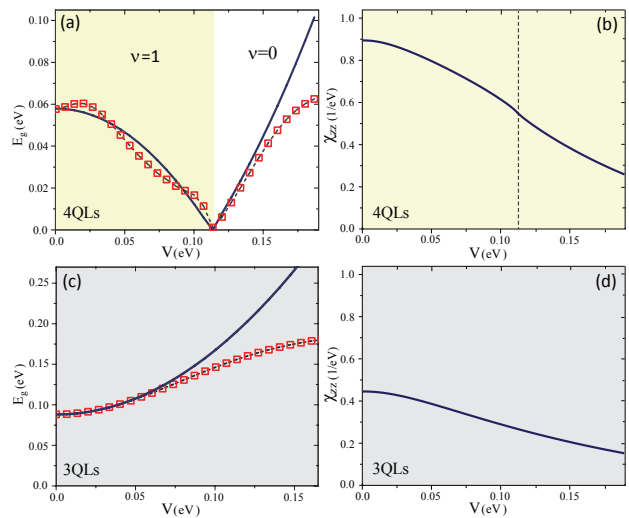


FIG. 2. (color online). Band structure and magnetic properties. (a), (c) Band gap of 4 QLs and 3 QLs TIs, respectively, as a function of inversion asymmetry  $V$ , calculated analytically from Eq. (1) (solid line) or numerically (symbols). The parameters are taken from Ref. [31] for  $(\text{Bi}_{0.1}\text{Sb}_{0.9})_2\text{Te}_3$ . In (a), when  $0 \leq V < V_c$ , the band structure is inverted, resulting in a topologically non-trivial QSH phase with  $Z_2$  index  $\nu = 1$ ;  $V > V_c$ , the band structure becomes normal. (b), (d) The calculated spin susceptibility vs  $V$  for 4 QLs and 3 QLs TIs, respectively.



$\Delta$  denotes the magnitude of FM exchange coupling along  $z$  axis, where the same effective  $g$  factor for two surface bands is assumed. In the absence of inversion symmetry breaking  $V = 0$ , the system will be in the QAH phase as long as the spin splitting exceeds the hybridization gap ( $|\Delta| > |m_0|$ ) [26]. In realistic materials, however, such condition is hard to achieve in 3 QLs due to weak FM order, thus 3 QLs is a NI. With strong FM order, QAH state is realized in 4 QLs [33]. We further consider the  $V \neq 0$  case. Similarly, we determine the phase boundaries by the gapless regions in the energy spectrum, which leads to the following two conditions: (i),  $m_0^2 + V^2 = \Delta^2$ ; or (ii),  $m(k) = 0$  and  $\Delta^2 + v_F^2 k^2 = V^2$ . The entire phase diagram for 4 QLs in the  $(\Delta, V)$  space is shown in Fig. 3. Except for the phase boundaries, there are four gapped phases. The NI A is a band insulator with zero charge Hall conductance, while the NI B is a band insulator with both spin Hall conductance and charge Hall conductance be nonzero and non-quantized. As predicted, the inversion symmetry breaking would induce the FM-to-PM transition, and with the PM order, the system would be in the NI state. Therefore, the electrical control of FM will drive the QAH-to-NI phase transition.

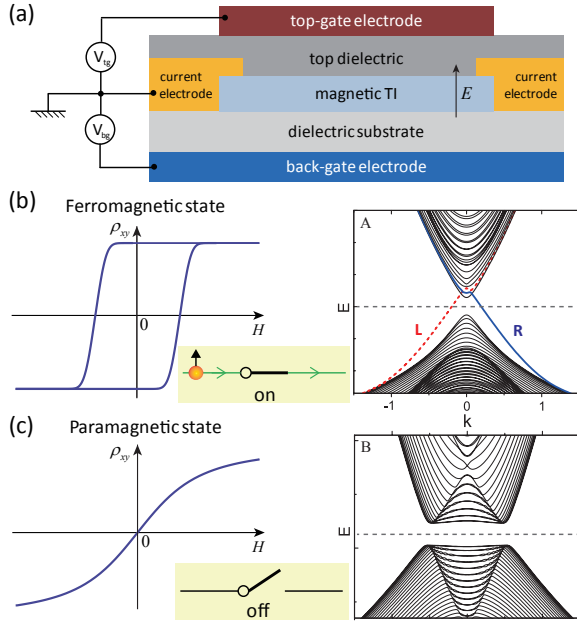


FIG. 4. (color online). Electrical manipulation of FM phase in a magnetic TI. (a) Schematic diagram of a proposed topological transistor device for using dual gates and an electric field to tune charge/spin transport.  $V_{tg}$ , top-gate voltage;  $V_{bg}$ , back-gate voltage. (b) Without an electric field, the magnetic TI film has FM order and is in a QAH phase, thus protected, chiral edge state (upper right). (c) Applying an electric field perpendicular to the film breaks the inversion symmetry, which drives the magnetic TI to be PM order and in a NI phase, thus no protected edge state (lower right).

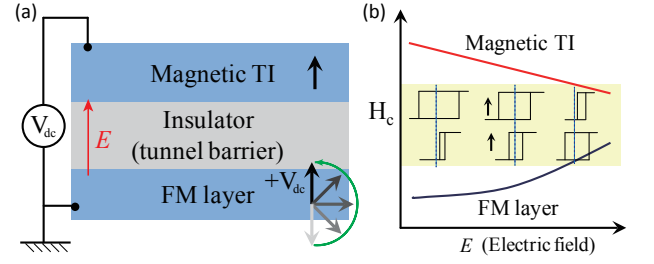


FIG. 5. (color online). Electric field assisted switching in a MTJ with magnetic TI on top layer. Such MTJ can be used as voltage based writing of MRAM with more energy-efficiency. (a) Schematic drawing of a MTJ and the effect of magnetic easy axis (black arrow) switching by an electric field. (b) Schematic on dependence of the coercivities for the top magnetic TI and bottom FM layers on electric field.

*Transistor device proposal* As shown in Fig. 4(b) and 4(c), in the QAH insulator, the metallic chiral edge states conduct without dissipation; while these states disappear in NI. Thus, edge state transport in the 2D magnetic TI has the unique property that the conductance is easily and widely tunable by an electric field instead of carrier depletion. This mechanism improves power efficiency and works at high on/off ratio. In the on state, the current is carried by the *dissipationless* edge states. To turn it off, only a local electric field is needed, which minimizes power consumption. The resistance of the off state depends on the amount of impurity states inside the energy gap, and thus the on/off ratio can be improved by controlling the film quality. On the other hand, even in the diffusive transport regime, the on/off ratio of the topological transistor can be further enhanced with a quantized on state conductance of  $e^2/h$  per edge and a negligible off state conduction. The above functionality motivates us to propose a *topological transistor* device made of dual-gated magnetic TI thin films, as shown in Fig. 4(a). Using the two gates, one can control the electric field across the film and the carrier density independently, and thus turn on and off the charge transport by purely electrical means functioning as a transistor.

*MRAM proposal* The coercivity  $H_c$  of magnetic TI films can be modified dramatically through the electric field applied at the film interface, as shown in Fig. 5(b). Such property of field-controlled FM in magnetic TIs can be used for voltage based writing of non-volatile magnetic random access memories (MRAM) in the magnetic tunnel junctions (MTJs). As proposed in Fig. 5, the magnetic TI is the top FM layer, and MgO and CoFeB are the insulator barrier layer and bottom FM layer, respectively. With opposite magnetic anisotropy in an electric field for magnetic TI and bottom FM layer, one can realize the electric-field-assisted reversible switching of FM in the MTJs [34]. Compared with the spin transfer torque effect, the magnetic configuration and magnetic tunnel-

ing magnetoresistance in MTJs can be manipulated by voltage pulses with much smaller current densities.

*Conclusion* We predict the field-controlled FM in magnetic TIs, which is expected to have a great impact for electronic applications of TIs. We would like to emphasize that the modulation of  $T_c$  in ferromagnet (In,Mn)As by an electric field is due the electric control of carrier concentration [35], while the modulation of  $T_c$  in magnetic TIs predicted here by an electric field is due to the electric control of band inversion and spin texture of band structures.

This work is supported by the US Department of Energy, Office of Basic Energy Sciences, Division of Materials Sciences and Engineering, under Contract No. DE-AC02-76SF00515 and the Defense Advanced Research Projects Agency Microsystems Technology Office, Meso-Dynamic Architecture Program (MESO) through the Contract No. N66001-11-1-4105, and in part by FAME, one of six centers of STARnet, a Semiconductor Research Corporation program sponsored by MARCO and DARPA.

- 
- [1] X.-L. Qi and S.-C. Zhang, *Rev. Mod. Phys.* **83**, 1057 (2011).
- [2] M. Z. Hasan and C. L. Kane, *Rev. Mod. Phys.* **82**, 3045 (2010).
- [3] X.-L. Qi, Y.-S. Wu, and S.-C. Zhang, *Phys. Rev. B* **74**, 085308 (2006).
- [4] X.-L. Qi, T. L. Hughes, and S.-C. Zhang, *Phys. Rev. B* **78**, 195424 (2008).
- [5] C.-X. Liu, X.-L. Qi, X. Dai, Z. Fang, and S.-C. Zhang, *Phys. Rev. Lett.* **101**, 146802 (2008).
- [6] R. Li, J. Wang, X. L. Qi, and S. C. Zhang, *Nat. Phys.* **6**, 284 (2010).
- [7] R. Yu, W. Zhang, H.-J. Zhang, S.-C. Zhang, X. Dai, and Z. Fang, *Science* **329**, 61 (2010).
- [8] A. Rüegg and G. A. Fiete, *Phys. Rev. B* **84**, 201103 (2011).
- [9] J. Wang, B. Lian, H. Zhang, Y. Xu, and S.-C. Zhang, *Phys. Rev. Lett.* **111**, 136801 (2013).
- [10] J. Wang, B. Lian, H. Zhang, and S.-C. Zhang, *Phys. Rev. Lett.* **111**, 086803 (2013).
- [11] M. Onoda and N. Nagaosa, *Phys. Rev. Lett.* **90**, 206601 (2003).
- [12] C.-Z. Chang, J. Zhang, X. Feng, J. Shen, Z. Zhang, M. Guo, K. Li, Y. Ou, P. Wei, L.-L. Wang, Z.-Q. Ji, Y. Feng, S. Ji, X. Chen, J. Jia, X. Dai, Z. Fang, S.-C. Zhang, K. He, Y. Wang, L. Lu, X.-C. Ma, and Q.-K. Xue, *Science* **340**, 167 (2013).
- [13] X. Kou, S.-T. Guo, Y. Fan, L. Pan, M. Lang, Y. Jiang, Q. Shao, T. Nie, K. Murata, J. Tang, Y. Wang, L. He, T.-K. Lee, W.-L. Lee, and K. L. Wang, *Phys. Rev. Lett.* **113**, 137201 (2014).
- [14] J. G. Checkelsky, R. Yoshimi, A. Tsukazaki, K. S. Takahashi, Y. Kozuka, J. Falson, M. Kawasaki, and Y. Tokura, *Nat. Phys.* **10**, 731 (2014).
- [15] K. F. Garrity and D. Vanderbilt, *Phys. Rev. B* **90**, 121103 (2014).
- [16] F. D. M. Haldane, *Phys. Rev. Lett.* **61**, 2015 (1988).
- [17] D. J. Thouless, M. Kohmoto, M. P. Nightingale, and M. den Nijs, *Phys. Rev. Lett.* **49**, 405 (1982).
- [18] J. G. Checkelsky, J. Ye, Y. Onose, Y. Iwasa, and Y. Tokura, *Nature Phys.* **8**, 729 (2012).
- [19] X. Kou, M. Lang, Y. Fan, Y. Jiang, T. Nie, J. Zhang, W. Jiang, Y. Wang, Y. Yao, L. He, and K. L. Wang, *ACS Nano* **7**, 9205 (2013).
- [20] Z. Zhang *et al.*, *Nature Commun.* doi: 10.1038/ncomms5915 (2014).
- [21] I. Žutić, J. Fabian, and S. Das Sarma, *Rev. Mod. Phys.* **76**, 323 (2004).
- [22] A. Fert, *Rev. Mod. Phys.* **80**, 1517 (2008).
- [23] T. Jungwirth, J. Sinova, J. Mašek, J. Kučera, and A. H. MacDonald, *Rev. Mod. Phys.* **78**, 809 (2006).
- [24] T. Dietl and H. Ohno, *Rev. Mod. Phys.* **86**, 187 (2014).
- [25] J. Zhang, C.-Z. Chang, P. Tang, Z. Zhang, X. Feng, K. Li, L.-L. Wang, X. Chen, C. Liu, W. Duan, K. He, Q.-K. Xue, X. Ma, and Y. Wang, *Science* **339**, 1582 (2013).
- [26] J. Wang, B. Lian, and S.-C. Zhang, *Phys. Rev. B* **89**, 085106 (2014).
- [27] Y. Zhang, K. He, C.-Z. Chang, C.-L. Song, L.-L. Wang, X. Chen, J.-F. Jia, Z. Fang, X. Dai, W.-Y. Shan, S.-Q. Shen, Q. Niu, X.-L. Qi, S.-C. Zhang, X.-C. Ma, and Q.-K. Xue, *Nature Phys.* **6**, 584 (2010).
- [28] Q. Liu, C.-X. Liu, C. Xu, X.-L. Qi, and S.-C. Zhang, *Phys. Rev. Lett.* **102**, 156603 (2009).
- [29] B. A. Bernevig, T. L. Hughes, and S. C. Zhang, *Science* **314**, 1757 (2006).
- [30] W.-Y. Shan, H.-Z. Lu, and S.-Q. Shen, *New J. Phys.* **12**, 043048 (2010).
- [31] H. Zhang, C.-X. Liu, X.-L. Qi, X. Dai, Z. Fang, and S.-C. Zhang, *Nature Phys.* **5**, 438 (2009).
- [32] C.-X. Liu, H. J. Zhang, B. Yan, X.-L. Qi, T. Frauenheim, X. Dai, Z. Fang, and S.-C. Zhang, *Phys. Rev. B* **81**, 041307 (2010).
- [33] K. He and Y. Wang, private communications.
- [34] W.-G. Wang, M. Li, S. Hageman, and C. L. Chien, *Nature Mater.* **11**, 64 (2011).
- [35] H. Ohno, D. Chiba, F. Matsukura, T. Omiya, E. Abe, T. Dietl, Y. Ohno, and K. Ohtani, *Nature* **408**, 944 (2000).